Hydrogenation studies on NdScSi and NdScGe

Tencé, Sophie; Mahon, Tadhg; Gaudin, Etienne; Chevalier, Bernard; Bobet, Jean-Louis; Flacau, Roxana; Heying, Birgit; Rodewald, Ute Ch.; Pöttgen, Rainer

Publisher's version / Version de l'éditeur:
http://doi.org/10.1016/j.jssc.2016.02.017
Journal of Solid State Chemistry, 2016-02-13

Journal of Solid State Chemistry ∎ (∎∎∎∎) ∎∎∎–∎∎∎

Contents lists available at ScienceDirect

Journal of Solid State Chemistry

journal homepage: www.elsevier.com/locate/jssc

Hydrogenation studies on NdScSi and NdScGe

Sophie Tencé [a,*], Tadhg Mahon [a], Etienne Gaudin [a], Bernard Chevalier [a], Jean-Louis Bobet [a], Roxana Flacau [b], Birgit Heying [c], Ute Ch. Rodewald [c], Rainer Pöttgen [c]

[a] CNRS, Université de Bordeaux, ICMCB, 87 Avenue Dr. A. Schweitzer, 33608 Pessac-Cedex, France
[b] Canadian Neutron Beam Centre, National Research Council Canada, Chalk River Laboratories, Building 459, Chalk River, Ontario, Canada K0J 1J0
[c] Institut für Anorganische und Analytische Chemie, Universität Münster, Corrensstraße 30, D-48149 Münster, Germany

ARTICLE INFO

Article history:
Received 17 November 2015
Received in revised form
12 February 2016
Accepted 13 February 2016

Keywords:
Silicides
Germanides
Crystal chemistry
Hydrogenation reactions
Neutron diffraction
Magnetic properties

ABSTRACT

NdScSi and NdScGe were synthesized from the elements via arc-melting and subsequent annealing. Their ordered La_2Sb type structures, with space group *I*4/*mmm*, were refined from single crystal X-ray diffractometer data: $a=428.94(6)$ and $b=1570.5(3)$ pm, $wR2=0.0395$, 309 F^2 values for NdScSi and $a=431.2(1)$ and $c=1581.3(5)$ pm, $wR2=0.1220$, 227 F^2 values for NdScGe, with 11 variables per refinement.

Hydrogen insertion was performed on both Nd-based intermetallics by solid/gas reaction. Hydrogen uptake keeps the pristine compound space group but yields an anisotropic expansion of the unit cell with a large increase of c ($\approx +7\%$) and a slight decrease of a ($\approx -1.7\%$) parameters. Hydrogen absorption at 350 °C and under 5 bar of H_2 pressure shows that the hydride $NdScSiH_{1.48(5)}$ is formed. An *in-situ* neutron diffraction study during the deuteration of NdScSi reveals for the first time in a CeScSi-type compound, the possibility to fill two interstitial sites with deuterium atoms, leading to the composition $NdScSiD_{1.5}$ for the deuteride adopting then the $La_2Fe_2Se_2O_3$-type structure.

From magnetization measurements, we evidence that hydrogenation strongly reduces the Curie temperature of NdScSi ($T_C=175$ K) and NdScGe ($T_C=194$ K) since $NdScSiH_{1.5}$ and $NdScGeH_x$ undergo a magnetic transition at 4 K and around 2 K, respectively.

1. Introduction

The tetragonal La_2Sb structure [1] is one of the basic structure types for intermetallic compounds [2]. Besides the binary series of RE_2Sb antimonides and RE_2Bi bismutides (*RE*=rare earth element), a larger variety of ternary rare earth-containing representatives of this structure are known, *e.g.* the series of *RE*ScSi silicides [3], *RE*ScGe germanides [4], and *RE*ScSb antimonides [5]. The distinctly smaller size of scandium allows for a complete ordering of the two rare earth sites leading to the formation of the CeScSi-type structure. Substitution of the antimony by the tetrels silicon and germanium permits for a certain electronic flexibility.

The silicides and germanides have been intensively studied with respect to their magnetic properties since several representatives exhibit comparatively high magnetic ordering temperatures: $T_N=26$ and 43 K for CeScSi and CeScGe [6–9], the 194 K ferromagnet NdScGe [10] or ferromagnetic TbScGe ($T_C=216$ K) [11]. The Curie temperatures of GdScSi (354 K) and GdScGe (349 K) are even above room temperature and both compounds show a moderate magnetocaloric effect [12].

Besides the high magnetic ordering temperature, the interest in the *RE*ScSi and *RE*ScGe compounds concerns their hydrogenation behavior. The larger rare earth atoms form layers of condensed tetrahedra that can be filled with hydrogen leading to the quaternary compounds *RE*ScSiH and *RE*ScGeH in compliance with the many ZrCuSiAs-type phases [13–15]. The hydrogen insertion has a drastic influence on the magnetic ground state. Recent examples are the pairs CeScSi/CeScSiH [16] and GdScGe/GdScGeH [17]. In both cases hydrogenation leads to a drastic decrease of the magnetic ordering temperature: (i) T_N decreases from 26 to 3 K from CeScSi to CeScSiH and (ii) the 350 K ferromagnet GdScGe switch to the 6 K antiferromagnet GdScGeH.

Based on these striking results we extended our systematic studies on the pairs of *RE*ScSi/*RE*ScSiH and *RE*ScGe/*RE*ScGeH compounds with respect to the neodymium representatives. So far, the ternaries have only been studied on the basis of powder diffraction data [3,4,10,18]. Herein we report on single crystal X-ray diffraction data for the precursor compounds NdScSi and NdScGe and hydrogenation/deuteration experiments with respect to changes in the magnetic ground state. In particular, we present *in-situ* neutron diffraction experiments of deuteration which evidence a new structural type of deuteride obtained from CeScSi-type compounds.

* Corresponding author.
E-mail address: sophie.tence@icmcb.cnrs.fr (S. Tencé).

http://dx.doi.org/10.1016/j.jssc.2016.02.017
0022-4596/

2. Experimental

2.1. Synthesis

Starting materials for the preparation of the NdScSi and NdScGe samples were neodymium ingots (Johnson-Matthey), scandium ingots (Johnson Matthey), silicon and germanium lumps (Alfa Aesar), all with stated purities higher than 99.9%. For NdScGe, the elements were weighed in the ideal 1:1:1 atomic ratio and arc-melted [19] three times under *ca.* 700 mbar argon pressure. Argon was purified with titanium sponge (900 K), silica gel, and molecular sieves. The arc-melted button was subsequently sealed in an evacuated silica tube and annealed at 1173 K for 14 days. For preparation of the NdScSi sample the starting composition was 0.95:1.05:1 in order to avoid formation of the $Nd_{2-x}Sc_{3+x}Si_4$ phase. After the arc-melting procedure the sample was annealed for a longer period, *i. e.* three weeks, at 1173 K. The resulting silvery ingots were stable in air over weeks.

Preliminary hydrogenation experiments were performed by solid–gas reaction in a stainless steel container hermetically sealed with a graphite joint. the annealed ingots were crushed and heated under vacuum at temperatures between 250 and 350 °C for 2 h and then exposed to 30 bar of hydrogen gas at the same temperature for 1.5 days. Indeed, below 250 °C residual pristine compound is still present and above 350 °C the container becomes no longer tight. The formed hydrides are stable in air.

Further hydrogen sorption kinetics were investigated by the use of an automatic sievert-type volumetric apparatus (HERA, hydrogen storage system) in the temperature range from 200 to 350 °C and with 5 bar of H_2 [20].

2.2. Scanning electron microscopy

The NdScSi and NdScGe crystals investigated on the diffractometers were studied by EDX using a Zeiss EVO MA10 scanning electron microscope with NdF_3, Sc, SiO_2, and Ge as standards for the semiquantitative measurements. No impurity elements have been detected. The conchoidal fracture of the crystals hampered quantitative analyses.

2.3. X-ray powder and single crystal data

The polycrystalline NdScSi and NdScGe samples were characterized through Guinier powder patterns (imaging plate technique, Fujifilm BAS–1800) with CuKα_1 radiation and α-quartz (a=491.30 and c=540.46 pm) as an internal standard. The tetragonal lattice parameters (Table 1) were refined from the powder diffraction data by a least-squares routine. Correct indexing of the patterns was ensured by intensity calculations [21] using the atomic parameters obtained from the structure refinements. Our data are in agreement with earlier literature results on NdScSi and NdScGe powders [3,4]. The hydride samples were analyzed with a Philips1050-diffractometer (CuKα radiation) and their cell parameters were determined by a full-pattern matching of the X-ray diffractogram using the Fullprof program [22].

Irregularly-shaped single crystals of NdScSi and NdScGe were selected from the crushed annealed samples and glued to thin quartz fibers. They were first investigated by Laue photographs on a Buerger camera (white molybdenum radiation, Fuji-film image plate technique) in order to check their quality for intensity data collection. The NdScSi data set was collected at room temperature by use of a four-circle diffractometer (CAD4) with graphite monochromatized MoKα radiation and a scintillation counter with pulse height discrimination. Scans were taken in the $\omega/2\theta$ mode. An empirical absorption correction was applied on the basis of Ψ-scan data, accompanied by spherical absorption corrections.

Table 1
Crystal data and structure refinement results of NdScSi and NdScGe with ordered La_2Sb type structure; space group $I4/mmm$; Z=4.

Compound	NdScSi	NdScGe
a, pm	428.94(6)	431.2(1)
c, pm	1570.5(3)	1581.3(5)
V, nm^3	0.2890	0.2940
Molar mass, g mol^{-1}	217.29	261.79
Calculated density, g cm^{-3}	5.00	5.91
Absorption coefficient, mm^{-1}	20.2	29.4
Diffractometer	CAD4	IPDS2
Detector distance, mm	–	60
Exposure time, min	–	30
ω range; increment, deg.	–	0–180, 1.0
Integr. param. A, B, EMS	–	12.5; 2.5; 0.010
F(000), e	380	452
Crystal size, μm^3	20 × 20 × 30	10 × 20 × 20
Transm. ratio (max/min)	1.57	2.04
θ range, deg.	2–40	4–35
Range in hkl	±7, ±7, ±28	±6, ±6, ±25
Total no. reflections	3564	2009
Independent reflections/R_{int}	309/0.0662	227/0.1921
Reflections with $I \geq 2\sigma(I)/R_\sigma$	298/0.0240	164/0.1011
Data/parameters	309/11	227/11
Goodness-of-fit on F^2	1.083	1.088
$R1/wR2$ for $I \geq 2\sigma(I)$	0.0172/0.0389	0.0574/0.1101
$R1/wR2$ for all data	0.0184/0.0395	0.0936/0.1220
Extinction coefficient	0.0031(6)	0.004(2)
Largest diff. peak /hole, e Å^{-3}	1.84/−2.30	2.78/−2.72

Intensity data of the NdScGe crystal were collected at room temperature by use of a Stoe IPDS-II imaging plate diffractometer in oscillation mode (graphite monochromatized Mo$K\alpha$ radiation). A numerical absorption correction was applied to the data set. All relevant crystallographic data and details of the data collections and evaluations are listed in Table 1.

The Guinier patterns of the NdScSi and NdScGe samples clearly indicated isotypism with the respective cerium compounds [16]. Analyses of the two data sets were in agreement with space group $I4/mmm$ and the positional parameters of CeScSi [16] were taken as starting values. Both structures were then refined with SHELXL-97 [23,24] (full matrix least squares on F_o^2) with anisotropic displacement parameters for all sites. The occupancy parameters have been refined in a separate series of least squares cycles. All sites were fully occupied within two standard deviations. Final difference Fourier synthesis revealed no significant residual peaks. The refined atomic parameters and interatomic distances are listed in Tables 2 and 3. For NdScGe we find excellent agreement with a recent neutron diffraction study [10].

Further details on the structure refinements are available. Details may be obtained from: Fachinformationszentrum Karlsruhe, D-76344 Eggenstein-Leopoldshafen (Germany), by quoting the Registry No's. CSD–427369 (NdScSi) and CSD–427370 (NdScGe).

2.4. Neutron diffraction experiments

In-situ neutron powder diffraction experiments of deuteration were performed on the C2 diffractometer at the Canadian Neutron Beam Centre (CNBC), using a wavelength of λ=1.328 Å (Si(531) monochromator). C2 is equipped with a curved 800-wire BF_3 position sensitive detector with a wire spacing of 0.1°. The experimental setup is designed so that the sample holder can be filled with hydrogen/deuterium gas up to 40 bar and heated in the 25–400 °C temperature range [25]. The FullProf Suite program was used for nuclear structure refinements using the Rietveld method [22].

Please cite this article as: S. Tencé, et al., J. Solid State Chem. (2016), http://dx.doi.org/10.1016/j.jssc.2016.02.017

Table 2
Atomic coordinates and equivalent isotropic displacement parameters (pm^2) of NdScSi, NdScGe and $NdScSiD_{1.5}$. U_{eq} is defined as one third of the trace of the orthogonalized U_{ij} tensor.

	Atom	Wyck.	*x*	*y*	*z*	U_{eq}/U_{iso}*	*Occup.*
NdScSi	Nd	4*e*	0	0	0.32347(1)	76(1)	1
	Sc	4*c*	0	1/2	0	91(1)	1
	Si	4*e*	0	0	0.12285(8)	80(2)	1
NdScGe	Nd	4*e*	0	0	0.3235(1)	141(5)	1
	Sc	4*c*	0	1/2	0	152(10)	1
	Ge	4*e*	0	0	0.1238(2)	143(7)	1
$NdScSiD_{1.47(3)}$	Nd	4*e*	0	0	0.316(1)	94(8)*	1
	Sc	4*c*	0	1/2	0	148(8)*	1
	Si	4*e*	0	0	0.109(1)	86(7)*	1
	D1	4*d*	0	1/2	1/4	195(17)*	1.01(1)
	D2	4*e*	0	0	0.518(1)	234(32)*	0.47(3)

The values marked with "*" correspond to U_{iso} parameters whereas the values without "*" correspond to U_{eq} parameters.

Table 3
Interatomic distances (pm), of NdScSi and NdScGe, calculated with the powder lattice parameters, and of $NdScSiD_{1.5}$ calculated with the neutron powder data. All distances within the first coordination spheres are listed. Standard deviations are all equal or less than 0.3 pm for NdScSi and NdScGe and equal or less than 2 pm for the deuteride.

NdScSi				**$NdScSiD_{1.5}$**			
Nd:	4	Si	314.8	Nd:	4	D1	233
	1	Si	315.1		1	D2	260
	4	Sc	350.5		1	D2	316
	4	Nd	381.1		4	Si	319
Sc:	4	Si	288.5		1	Si	325
	4	Sc	303.3		4	Sc	356
	4	Nd	350.5		4	Nd	361
Si:	4	Sc	288.5	Sc:	4	D2	211
	4	Nd	314.8		4	Si	270
	1	Nd	315.1		4	Sc	296
					4	Nd	356
NdScGe				Si:	4	Sc	270
Nd:	1	Ge	315.9		4	D1	304
	4	Ge	316.1		4	Nd	319
	4	Sc	352.6		1	Nd	324
	4	Nd	383.5	D1:	4	Nd	233
Sc:	4	Ge	291.2		4	D1	296
	4	Sc	304.9		4	Si	304
	4	Nd	352.6	D2:	1	D2	56
Ge:	4	Sc	291.2		4	Sc	211
	1	Nd	315.9		1	Nd	260
	4	Nd	316.1		1	Nd	316

2.5. Magnetization measurements

The magnetic properties of the hydrides were determined using a SQUID magnetometer from Quantum Design operating between 1.8 and 300 K and with fields up to 7 T.

3. Result and discussion

3.1. Crystal chemistry

The crystal chemistry of NdScSi and NdScGe is similar. In the following discussion we focus on the structure of the silicide. The main difference concerns the slightly larger germanium atoms which induce a slight, overall increase of the interatomic distances. The NdScSi structure is exemplarily shown in Fig. 1. It consists of two basic building units. The scandium and silicon atoms form $Sc_{4/2}Si_2$ empty octahedra which are condensed in *ab* direction by common scandium corners. Due to the body-centred space group, the [ScSi] layers around $z=1/2$ are shifted by $a/2+b/2$. The Sc–Si distances within the slightly compressed $Sc_{4/2}Si_2$ octahedra are 289 pm, slightly longer than the sum of the covalent radii for scandium and silicon of 261 pm [26]. Such Sc–Si distances typically occur in ternary scandium silicides, *e. g.* 281–286 pm in $Sc_4Pt_7Si_2$ [27] or 271–292 pm in Sc_3PtSi_3 [28].

The scandium atoms form square grids at $z=0$ and $z=1/2$ with Sc–Sc distances of 303 pm, somewhat shorter than in *hcp* scandium (6×325 and 6×331 pm) [29]. We can therefore assume significant Sc–Sc bonding for these octahedral edges. Similar short Sc–Sc distances have also been observed in Sc_3C_4 (314 pm) [30], $Sc_4Pt_7Si_2$ (305 pm) [27], and Sc_3Ru_2Mg (309 pm) [31].

The layers of condensed $Sc_{4/2}Si_2$ octahedra are separated by layers of edge-sharing $Nd_{4/4}$ tetrahedra. The stacking sequence of these layers is ABA'B', where the prime accounts for the $a/2+b/2$ shift and the mirror planes multiplying the layers. Within the neodymium based layers the Nd–Nd distances are at 381 pm, slightly longer than the average Nd–Nd distance of 368 pm in elemental neodymium with an ABAC stacking sequence [29]. The layers of condensed rare earth tetrahedra are similar to the many ZrCuSiAs type pnictide oxides [14], where they are filled by oxygen atoms. In NdZnSbO [32] the Nd–Nd distances are at 368 pm. The two alternating layer types in NdScSi are held together by Nd–Si interactions with Nd–Si distances of 315 pm. The latter are comparable to Nd_2ScSi_2 (Mo_2FeB_2 type; 301–309 pm Nd–Si) [18].

The neodymium coordination is presented at the right-hand part of Fig. 1. Each neodymium atoms is coordinated by five silicon (315 pm Nd–Si), four scandium (351 pm Nd–Sc) and four neodymium atoms (381 pm Nd–Nd).

3.2. Hydrogenation

The X-Ray diffraction (XRD) patterns of the pristine compound NdScSi and the hydride $NdScSiH_x$ are presented in Fig. 2. It clearly shows a change in the unit cell parameters. More precisely, a full pattern matching of the diffractograms indicates that the hydrogenation of NdScSi (or NdScGe) keeps the initial space group *I*4/*mmm*, the *a* parameter decreasing from 428.94(6) to 422.1(1) pm (−1.6%) and the *c* parameter increasing from 1570.5(3) to 1692.8 (2) pm (+7.8%). This anisotropic volume change yields a volume cell expansion of 4.0% and a strong augmentation of the *c*/*a* ratio of 9.8%. A similar tendency is observed for the isotypic germanide since the unit cell parameters change from $a=431.2(1)$ and $c=1581.3(5)$ pm to $a=423.4(2)$ and $c=1680(9)$ pm. However, the hydrogenation of NdScGe is more difficult to achieve as we notice a significant broadening of some reflections such as the (103) or (105) line. This may be related to the larger size of the germanium atom with respect to the silicon one in addition to the repulsive interaction between the H and *X* atoms (*X*=Si, Ge). Such repulsive interactions have already been reported, for example, in $La_3Pd_5SiD_x$ deuterides [33] or in *RETX*H hydrides (*RE*=rare earth, *T*=transition metal) in which strong displacements of Si atoms are observed upon hydrogenation [34–36].

It is worthwhile to point out that modification of the temperature of H_2 absorption led to slightly different lattice parameters, *i. e.* higher *c* parameters and lower *a* parameters are observed when the temperature of hydrogenation increases. This suggested the existence of probably more than one interstitial site for hydrogen and/or the existence of a homogeneity range. Indeed, in the case of CeFeSi-type intermetallics, hydrogenation leads to stoichiometric ZrCuSiAs-type hydrides with only one site, the $Ce_{4/4}$ tetrahedra, fully occupied by hydrogen [34–37]. As a result, we

Please cite this article as: S. Tencé, et al., J. Solid State Chem. (2016), http://dx.doi.org/10.1016/j.jssc.2016.02.017

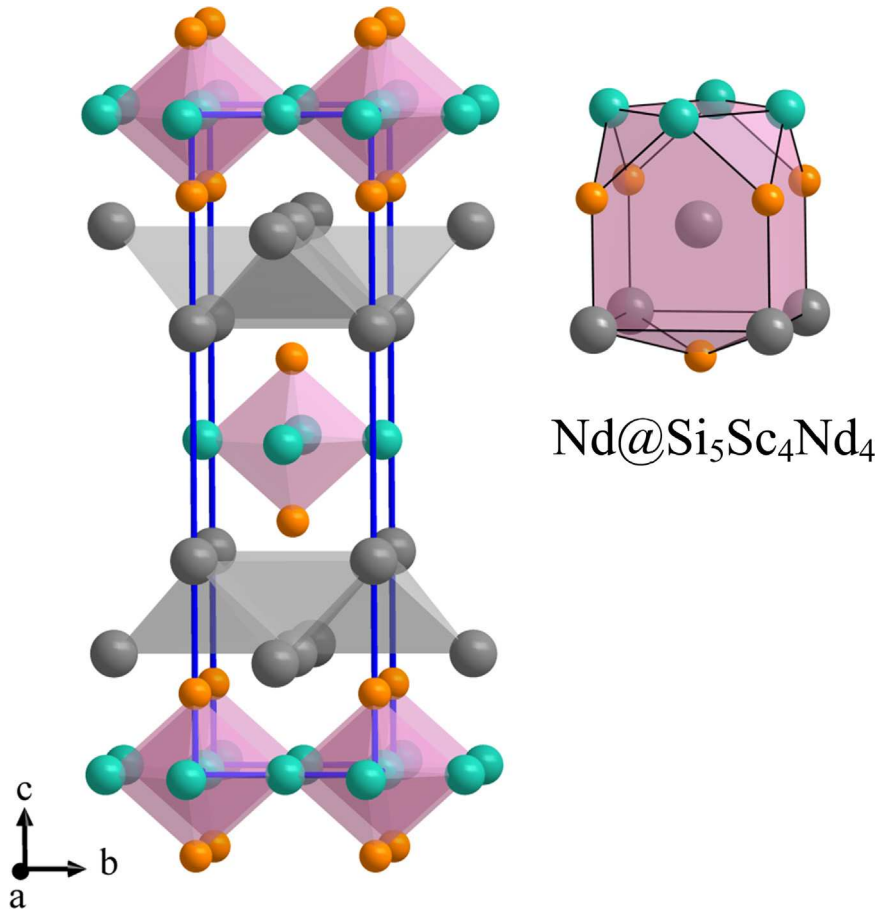

Fig. 1. Left: The unit cell of NdScSi. Neodymium, scandium, and silicon atoms are drawn as dark gray, green, and orange balls, respectively. The layers of corner-sharing $Sc_{4/2}Si_2$ octahedra and edge-sharing $Nd_{4/4}$ tetrahedra are emphasized. Right: coordination of the neodymium atoms. (For interpretation of the references to color in this figure legend, the reader is referred to the web version of this article.)

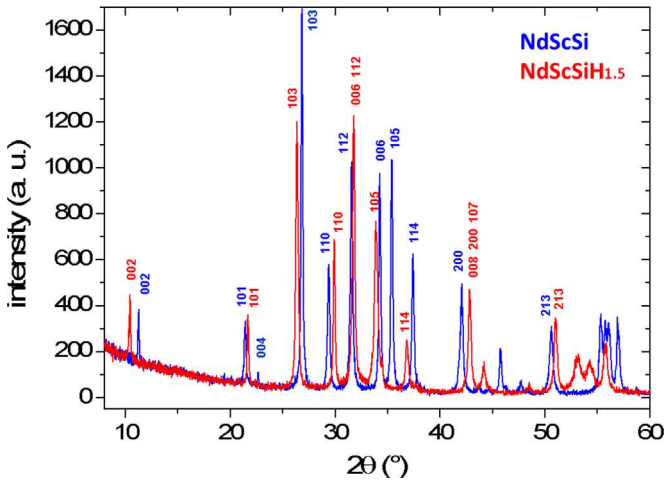

Fig. 2. X-ray diffraction patterns of NdScSi and $NdScSiH_{1.5}$ at room temperature. The main (*hkl*) lines are indicated to observe unit cell parameters modifications.

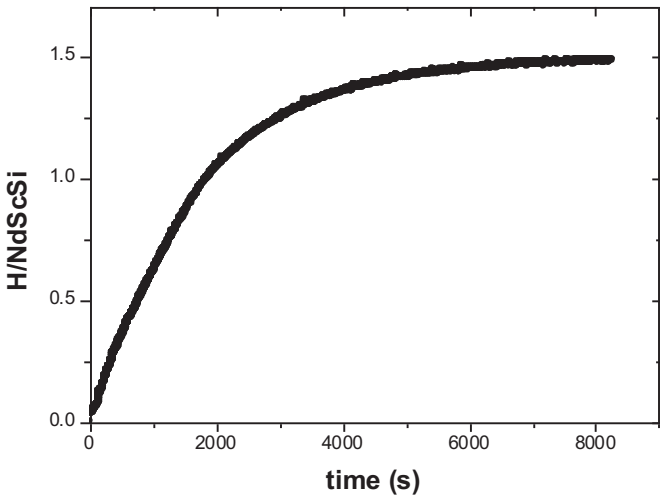

Fig. 3. Kinetics of hydrogen absorption in NdScSi at 350 °C and 5 bar.

always observe the same unit cell values, whatever the hydrogenation conditions are. For NdScSi and NdScGe, we assumed that, in addition to the tetrahedral $Nd_{4/4}$ site, a second interstice was partly filled by hydrogen atoms.

In order to check the above mentioned assumption and determine the hydrogen amount in the hydride, we performed hydrogen absorption measurement with a Sievert type apparatus. The sample was activated at 250 °C under primary vaccum for 2 h and then heated at 350 °C. When the temperature was stable for 10 min, hydrogen was introduced until reaching a pressure of 5 bar (e.g. within less than 10 s). As seen in Fig. 3, this first absorption leads to the formation of $NdScSiH_{1.48(5)}$ after about 2 h. It is worth pointing out that the kinetics can be influenced by the grains sizes, the particles sizes or even the ageing of the sample and then should not be considered as an intrinsic data. Nevertheless, the maximum absorbed hydrogen is an intrinsic data. The H amount confirms that the $Nd_{4/4}$ tetrahedron is not the only site filled by hydrogen atoms. To better clarify the hydrogenation process and

Please cite this article as: S. Tencé, et al., J. Solid State Chem. (2016), http://dx.doi.org/10.1016/j.jssc.2016.02.017

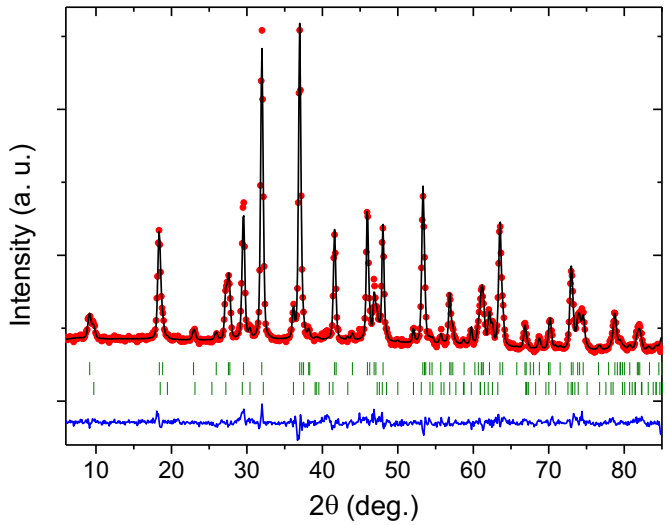

Fig. 4. Refinement of the neutron powder diffraction pattern recorded at room temperature after 15 h of deuteration of NdScSi. The upper and lower ticks correspond to the deuteride and NdScSi, respectively.

solve the hydride crystal structure, neutron diffraction measurements were performed during the deuteration of the NdScSi silicide.

3.3. *In-situ neutron diffraction study*

The *in-situ* deuteration was performed at 5 bar from room temperature to 400 °C, temperature above which the vanadium sample holder is no longer tight. Upon heating, additional nuclear peaks appear in Bragg positions slightly shifted from those of NdScSi. This corresponds to the appearance of the deuterated phase which coexists with the parent compound. After 15 h of heating under 5 bar of D_2 and up to 350 °C, a small amount of the pristine compound is still present (*ca.* 13 wt%) as visible on the diffractogram of the Fig. 4 recorded at room temperature. All extra peaks are indexed with the tetragonal space group *I*4/*mmm* suggesting that $NdScSiD_x$ adopts a stuffed CeScSi-type structure upon deuteration. We observe a slight decrease of the *a* parameter from 428.37(1) to 418.75(6) pm (−2.2%) and a strong increase of the *c* parameter from 1568.7(1) to 1663.1(3) pm (+6.0%). The Rietveld refinement of the data taking into account both phases confirms that deuterium atoms are localized in two Wyckoff positions. Indeed, as observed for CeFeSi-type compounds, deuterium atoms completely occupy the $Nd_{4/4}$ tetrahedral site in D1 (0 1/2 1/4). Additionally, D-atoms also occupy $NdSc_{4/4}$ square based pyramidal sites in D2 (0 0 0.518(1)). Indeed, a better refinement is obtained when D2-atoms are slightly shifted from the Sc_4 square plane towards the Nd-atom (see Section 3.4 below). This site is only half filled since otherwise it would induce too small interatomic distances between D2-atoms, i.e. D2 − D2 = 56(2) pm. Thus, the deuteride adopts the $La_2Fe_2Se_2O_3$-type structure [38]. Details of the crystal structure and interatomic distances are gathered in Tables 2 and 3 and the crystal structure is drawn in Fig. 5. After 26 h of heating under 5 bar of D_2 and up to 400 °C the parent phase NdScSi has completely disappeared and only the peaks of the deuteride are present. The refinement of the structure yields the same structural parameters as determined previously. So, under these conditions of deuteration, $NdScSiD_{1.5}$ is formed, in fair agreement with the hydrogen absorption measurement. Both interstitial sites are filled simultaneously since no intermediate deuteride is observed during both *in-situ* experiment and hydrogen absorption measurement. Besides, the study has shown that

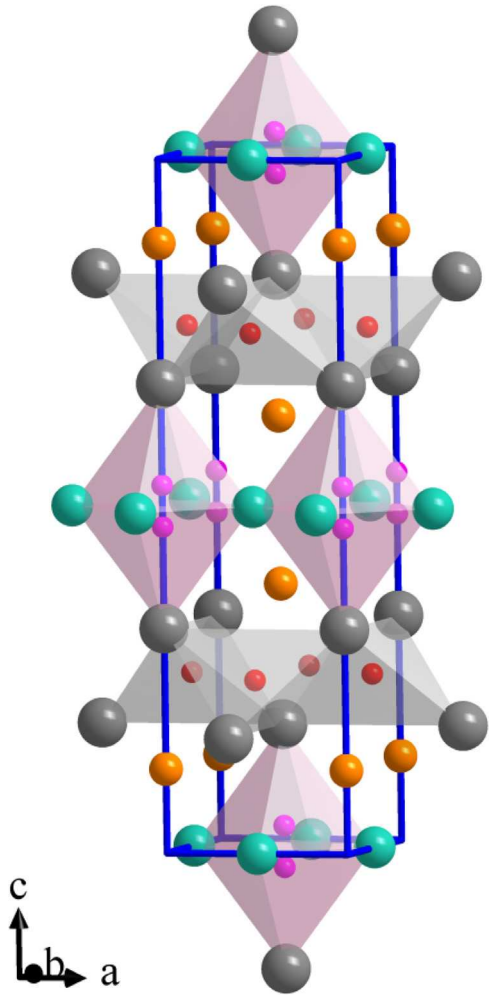

Fig. 5. Unit cell of $NdScSiD_{1.5}$. Nd, Sc, Si, D1 and D2 atoms are drawn as dark gray, green, orange, red and pink balls, respectively. The $Nd_{4/4}$ tetrahedra and the $NdSc_{4/4}$ square based pyramids containing D1 and D2, respectively, are emphasized. (For interpretation of the references to color in this figure legend, the reader is referred to the web version of this article.)

the deuteride is stable under ambient conditions or under vacuum.

3.4. *Structural discussion*

The deuteration (or hydrogenation) of NdScSi increases the compactness of the [Nd] and [ScSi] layers and the distance between them. This latter, which is equal to *c*/4, increases from 393 to 416 pm. The two-dimensional character of the substructures is then reinforced. In the [Nd] layer the Nd–Nd distances range from 381 to 361 pm for the shortest one (see Table 3) and from 429 to 419 pm for the longest one (these last two values correspond to the length of the *a*-axis). In the other layer the Sc–Si distances are decreasing from 289 to 270 pm and the Sc–Sc distances from 303 to 296 pm. The distance between the position in the center of the tetrahedron and the Nd-atom decreases from 244 to 233 pm after hydrogenation and this last value (Nd–D1 distance, see Table 3) is close to the Nd–H distance, 237 pm, in NdH_2 [39]. The other interstitial site filled by hydrogen (or deuterium) is located in the $Sc_{4/2}Nd_2$ octahedron. This position has been observed in the homologous phases $La_2Ti_2As_2H_{2.3}$ [40], $Ti_2SbD_{0.5}$ [41] and Sr_4Bi_2O [42] for instance. In the case of $La_2Ti_2As_2H_{2.3}$ and $Ti_2SbD_{0.5}$, the H- or D-atoms have been placed in the Wyckoff position 2*b* in the center of the octahedron with a huge value of the anisotropic displacement parameter U_{33}. In the case of Sr_4Bi_2O a splitting of

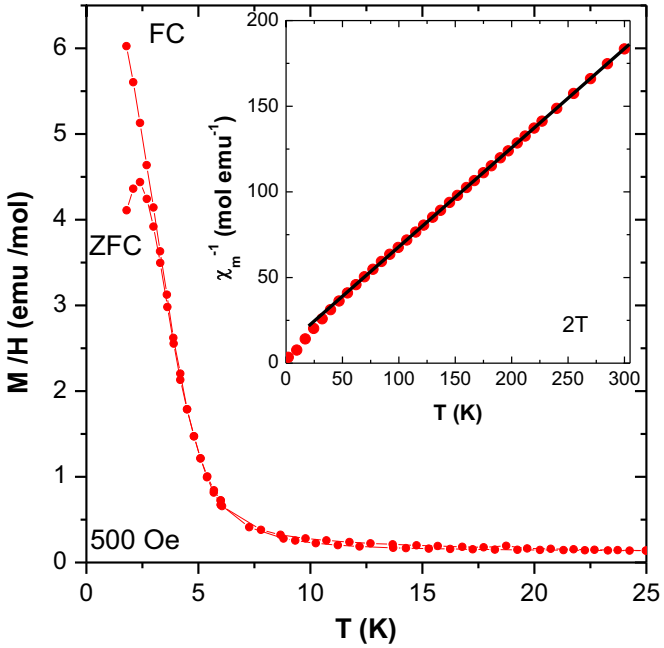

Fig. 6. Temperature dependance of the magnetization for $NdScSiH_{1.5}$ after zero field cooling (ZFC) and field cooling (FC). The inset shows the inverse of the susceptibility at 2 T with the Curie–Weiss fit in solid line.

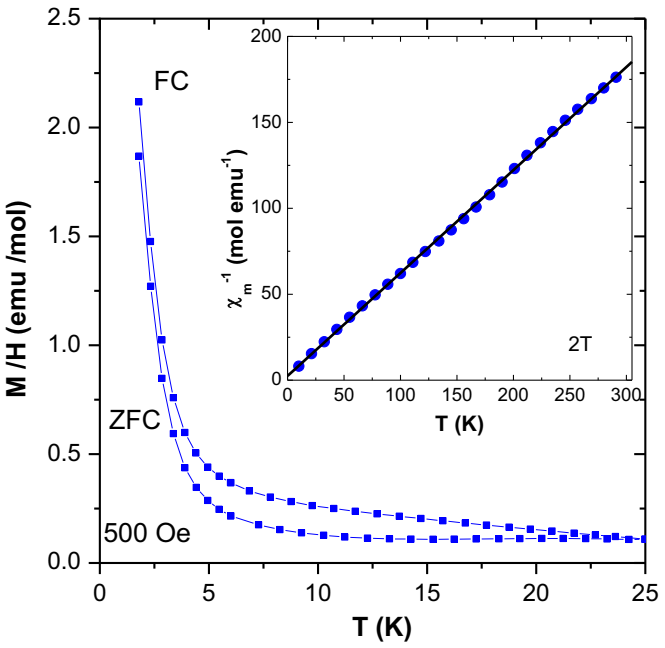

Fig. 7. Temperature dependance of the magnetization for $NdScGeH_x$ after zero field cooling (ZFC) and field cooling (FC). The inset shows the inverse of the susceptibility at 2 T with the Curie–Weiss fit in solid line.

this position has been considered, as it has been done in this work. For the D2 position, slightly displaced away from the Sc_4 plane, the Sc–D2 and Nd–D2 distances are equal to 211 and 260 pm, respectively. The Sc–D2 distance is close to the Sc–H distance, 207 pm, observed in ScH_2 [43]. If one considers the D2 position in the center of the $Sc_{4/2}Nd_2$ octahedron, this distance will only slightly decrease down to 209 pm. Thus the delocalization of the hydrogen (or deuterium) along the *c*-axis cannot be attributed to steric strains. It may also be noticed that in the case of $Ti_2SbD_{0.5}$ only the octahedral site is filled by H-atoms [41]. This induces a small increase of the *a* parameter (+0.9%) and a small decrease of the *c* parameter (−1.2%). The opposite evolution of the cell parameters observed after hydrogenation of NdScSi means that this evolution is mainly induced by the filling of the Nd_4 tetrahedra by H-atoms.

3.5. Magnetic properties

The pristine ternary compounds NdScSi and NdScGe undergo ferromagnetic order around $T_C = 175$ K [10] and $T_C = 194$ K, respectively [44]. The thermomagnetic measurements at 500 Oe of the hydrides $NdScSiH_{1.5}$ and $NdScGeH_x$ are presented in Figs. 6 and 7, respectively. The inverse of the susceptibility (inset of Figs. 6 and 7) follows a Curie–Weiss behavior, above 25 K for $NdScSiH_{1.5}$ and in the whole temperature range for $NdScGeH_x$. For the last one, a small anomaly is detected around 200 K which is due to the presence of residual non-hydrided pristine NdScGe in the sample. The effective moments are found to be equal to 3.71 μ_B and 3.65 μ_B for X=Si and Ge, respectively, i.e. in agreement with the free ion value of Nd^{3+} (3.62 μ_B). The paramagnetic Curie temperatures amount to $\theta_p = -16$ K and $\theta_p = -4$ K for $NdScSiH_{1.5}$ and $NdScGeH_x$, respectively.

At lower temperatures, $NdScSiH_{1.5}$ undergoes a magnetic transition at around 4 K, below which the Zero-Field-Cooled (ZFC) and the Field-Cooled (FC) curves deviate from each other (Fig. 6). In particular, the ZFC curve shows a maximum whereas the FC curve only presents an inflection point with decreasing temperature, indicating strong magnetocrystalline anisotropy in the

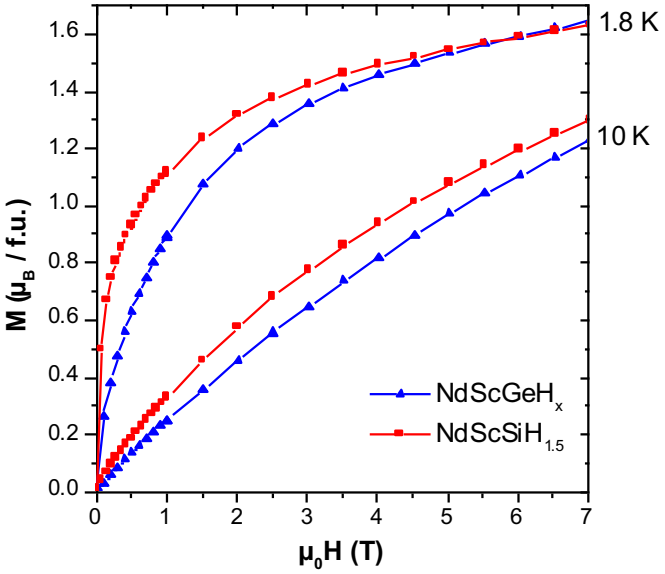

Fig. 8. Magnetization versus magnetic field at 1.8 and 10 K for $NdScSiH_{1.5}$ and $NdScGeH_x$.

hydride. The behavior of the field dependence of the magnetization at 1.8 K (Fig. 8) suggests the presence of a ferromagnetic component in $NdScSiH_{1.5}$. However, looking at the slightly negative paramagnetic Curie temperature, it is possible that the hydride is not strictly a ferromagnet but rather a ferrimagnet or a canted antiferromagnet. The other hypothesis is the presence of a spin–glass system which would be consistent with the deviation between the ZFC and the FC curve. Measurements of the frequency dependence of the AC susceptibility would be helpful. However, the magnetic transition is so close to the minimum temperature reached with our magnetometer, that such measurements are difficult. On the M(H) curve (Fig. 8) the saturation is not completely reached at 7 T but the magnetization tends to almost 1.7 μ_B per Nd atom. This value is close to that measured for the pristine

Please cite this article as: S. Tencé, et al., J. Solid State Chem. (2016), http://dx.doi.org/10.1016/j.jssc.2016.02.017

compound, *i.e.* 2 μ_B/Nd [44] but lower than the Nd^{3+} free ion value of 3.27 μ_B. The reduction of the moment could be ascribed to the crystal electric field effect which splits the $(2J+1)$ fold degenerated level of the free ion but also to the fact that the hydride is not purely ferromagnetic and thus not fully saturated at 7 T.

The susceptibility measurement of $NdScGeH_x$, shown in Fig. 7, does not evidence any clear magnetic transition down to 1.8 K since the ZFC and FC curves just increase at low temperatures. However, the magnetization *vs* field curve at 1.8 K (Fig. 8) presents a sharp increase at low field with a negative curvature. This behavior, similar to that of $NdScSiH_{1.5}$, evidences a ferromagnetic component for the Ge based hydride with a Curie temperature most likely around 2 K. It is noteworthy that this result is intrinsic, not due to the residual pristine compound (T_C = 194 K), since the isothermal M(H) curves at higher temperatures are linear at low fields (Fig. 8). However, as for the Si analog, the exact nature of the magnetic transition remains unclear so far.

Finally, the hydrogenation of the ternaries NdScSi and NdScGe yields a drastic reduction of the ordering temperature from 175 to 4 K for the silicide and from 194 K to approximately 2 K for the germanide. This result is very similar to that observed previously for CeScGe [16], GdScGe [17] or GdTiGe for which hydrogen insertion completely destroys the long range ferromagnetic order [45]. Density Functional Theory (DFT) calculations would be helpful to explain such a change in the magnetic properties, notably to determine the role of the electronic effect of H-atom insertion *versus* that of volume cell expansion.

4. Conclusion

We have shown that it is possible to insert hydrogen in the ternary intermetallics NdScSi and NdScGe. This induces a strong anisotropic volume cell expansion with a high increase of the *c* parameter whereas *a* decreases slightly. According to the hydrogenation absorption measurement, the hydride $NdScSiH_{1.5}$ is obtained. This result is confirmed by *in-situ* neutron diffraction experiments upon deuteration, which shows unambiguously that it adopts the $La_2Fe_2Se_2O_3$-type structure with two crystallographic sites occupied by hydrogen/deuterium atoms. To our knowledge, it is the first time that such hydride/deuteride is formed upon H/D insertion in a CeScSi-type intermetallic. Magnetization measurements have evidenced a strong reduction of the Curie temperature after hydrogenation for both intermetallics. Indeed, the magnetic ordering temperature decreases from 175 to 4 K for the silicide and from 194 to about 2 K for the germanide. However, despite the clear presence of a ferromagnetic component in both hydrides, the exact nature of the magnetic ground state will have to be further clarified. DFT calculations will be helpful to confirm the stabilization of the structure by the splitting of the D2-atom position from the center of the $Sc_{4/2}Nd_2$ octahedron. Besides, it will allow understanding the drastic influence of hydrogenation on the magnetic properties, in particular to precise the role of hydrogen insertion on the electronic structure modifications in respect to volume expansion effect.

Acknowledgments

This work was financially supported by the Deutsche Forschungsgemeinschaft through SPP 1458 *Hochtemperatursupraleitung in Eisenpnictiden*.

References

[1] W.N. Stassen, M. Sato, L.D. Calvert, Acta Crystallogr. B 26 (1970) 1534.
[2] P. Villars, K. Cenzual, Pearson's Crystal Data-Crystal Structure Database for Inorganic Compounds, ASM International, Materials Park, Ohio, USA, 2013 (release 2013/14).
[3] I.R. Mokra, O.I. Bodak, Dopov. Akad. Nauk Ukr. RSR (Ser. A), 1979, p. 312.
[4] O.I. Bodak, Z.M. Kokhan, Inorg. Mater. 19 (1984) 987.
[5] J. Nuss, M. Jansen, Z. Anorg, Allg. Chem. 640 (2014) 713.
[6] P.C. Canfield, J.D. Thompson, Z. Fisk, J. Appl. Phys. 70 (1991) 5992.
[7] Y. Uwatoko, T. Ishii, G. Oomi, H. Takahashi, N. Mōri, S. Nimori, G. Kido, J. L. Sarrao, D. Mandrus, Z. Fisk, J.D. Thompson, Phys. B 237–238 (1997) 207.
[8] S. Singh, S.K. Dhar, C. Mitra, P. Paulose, P. Manfrinetti, A. Palenzona, J. Phys.: Condens. Matter 13 (2001) 3753.
[9] S.N. Mishra, J. Phys.: Condens. Matter 21 (2009) 115601.
[10] J.M. Cadogan, D.H. Ryan, R. Gagnon, C.J. Voyer, J. Appl. Phys. 97 (2005) 10A916.
[11] P. Manfrinetti, A.V. Morozkin, O. Isnard, P. Henry, A. Palenzona, J. Alloy. Compd. 450 (2008) 86.
[12] S. Couillaud, E. Gaudin, V. Franco, A. Conde, R. Pöttgen, B. Heying, U. Ch Rodewald, B. Chevalier, Intermetallics 19 (2011) 1573.
[13] D. Johrendt, R. Pöttgen, Angew. Chem. Int. Ed. 47 (2008) 4782.
[14] R. Pöttgen, D. Johrendt, Z. Naturforsch. 63b (2008) 1135.
[15] D.C. Johnston, Adv. Phys. 59 (2010) 803.
[16] B. Chevalier, W. Hermes, B. Heying, U. Ch Rodewald, A. Hammerschmidt, S. F. Matar, E. Gaudin, R. Pöttgen, Chem. Mater. 22 (2010) 5013.
[17] S. Tencé, E. Gaudin, S. F. Matar, R. Pöttgen, B. Chevalier, Conference Report, SCTE-14.
[18] O.E. Banakh, B. Ya. Kotur, J. Alloy. Compd. 268 (1998) L3.
[19] R. Pöttgen, Th. Gulden, A. Simon, GIT Labor-Fachz 43 (1999) 133.
[20] R. Schulz, S. Boily, J. Huot, Apparatus for Titration and Circulation of Gases and Circulation of an Absorbent or Adsorbent Substance. Patent 09/424, 1999, p. 331.
[21] K. Yvon, W. Jeitschko, E. Parthé, J. Appl. Crystallogr. 10 (1977) 73.
[22] J. Rodriguez-Carvajal, Phys. B 192 (1993) 55.
[23] G.M. Sheldrick, SHELXL−97 – A Program for Crystal Structure Refinement, University of Göttingen, Germany, 1997.
[24] G.M. Sheldrick, Acta Crystallogr. A64 (2008) 112.
[25] R. Flacau, J. Bolduc, T. Bibienne, J. Huot, H. Fritzsche, J. Appl. Crystallogr. 45 (2012) 902.
[26] J. Emsley, The Elements, Oxford University Press, Oxford, 1999.
[27] T. Harmening, L. van Wüllen, H. Eckert, U. Ch Rodewald, R. Pöttgen, Z. Anorg. Allg. Chem. 636 (2010) 972.
[28] T. Harmening, D. Mohr, H. Eckert, A. Al Alam, S.F. Matar, R. Pöttgen, Z. Anorg. Allg. Chem. 636 (2010) 1839.
[29] J. Donohue, The Structures of the Elements, Wiley, New York, USA, 1974.
[30] R. Pöttgen, W. Jeitschko, Inorg. Chem. 30 (1991) 427.
[31] M. Kersting, O. Niehaus, R.-D. Hoffmann, U.C. Rodewald, R. Pöttgen, Z. Kristallogr. 229 (2014) 285.
[32] I. Schellenberg, T. Nilges, R. Pöttgen, Z. Naturforsch. 63b (2008) 834.
[33] Y.O. Tokaychuk, Y.E. Filinchuk, D. Sheptyakov, K. Yvon, Inorg. Chem. 47 (2008) 6303.
[34] B. Chevalier, E. Gaudin, S. Tencé, B. Malaman, J. Rodriguez Fernandez, G. André, B. Coqblin, Phys. Rev. B 77 (2008) 014414.
[35] S. Tencé, G. André, E. Gaudin, P. Bonville, A.F. Al Alam, S.F. Matar, W. Hermes, R. Pöttgen, B. Chevalier, J. Appl. Phys. 106 (2009) 033910.
[36] S. Tencé, S.F. Matar, G. André, E. Gaudin, B. Chevalier, Inorg. Chem. 49 (2010) 4836.
[37] B. Chevalier, S. Tencé, E. Gaudin, S.F. Matar, J.-L. Bobet, J. Alloy. Compd. 480 (2009) 43.
[38] J.M. Mayer, L.F. Schneemeyer, T. Siegrist, J.V. Waszczak, B. Van Dover, Angew. Chem. Int. Ed. Engl. 31 (1992) 1645.
[39] W.L. Korst, J.C. Warf, Inorg. Chem. 5 (1966) 1719.
[40] H. Mizoguchi, S.W. Park, H. Hiraka, K. Ikeda, T. Otomo, H. Hosono, Angew. Chem. Int. Ed. 54 (2015) 2932.
[41] H. Wu, A.V. Skripov, T.J. Udovic, J.J. Rush, S. Derakhsh, H. Kleinke, J. Alloy. Compd. 496 (2010) 1.
[42] M. Wied, J. Nuss, W. Hönle, H.G. von Schnering, Z. Krist. NCS 226 (2011) 437.
[43] Yu. P. Khodyrev, R.V. Baranova, Kristallografiya 25 (1980) 172.
[44] S. Singh, S.K. Dhar, P. Manfrinetti, A. Palenzona, D. Mazzone, J. Magn. Magn. Mater. 269 (2004) 113.
[45] E. Gaudin, S.F. Matar, R. Pöttgen, M. Eul, B. Chevalier, Inorg. Chem. 50 (2011) 11046.